

4. Webster, P. J., Holland, G. J., Curry, J. A. and Chang, H. R., Changes in tropical cyclone number, duration, and intensity in a warming environment. *Science*, 2005, **309**, 1844–1846.
5. United Nations Disaster Relief Coordinator, Natural disasters and vulnerability analysis. Report of expert group meeting, UNDRO, Geneva, 1979; <http://unisdr.org/files/resolutions/NL800388.pdf>
6. UNDP-BCPR, Reducing disaster risk: a challenge for development. United Nations Development Programme – Bureau for Crisis Prevention and Recovery, New York, 2004; <http://www.undp.org/bcpr/disred/rdr.htm>
7. Turner, B. L. *et al.*, A framework for vulnerability analysis in sustainability science. *Proc. Natl. Acad. Sci. USA*, 2003, **100**, 8074–8079.
8. Joshi, P. C., Kishitawal, C. M., Simon, B. and Narayanan, M. S., Impact of ERS-1 scatterometer data in medium range forecasting (cyclone and monsoon), ISRO Scientific Report, 1998, ISRO-SAC-SR-43-98.
9. Roy, P. S., Dwivedi, R. S. and Vijayan, D., Remote sensing applications. National Remote Sensing Centre, ISRO, Hyderabad, 2012.
10. United Nations Development Programme – Asia-Pacific Development Information Programme (UNDP-APDIP) and Asian and Pacific Training Centre for Information and Communication Technology for Development (APCICT), 2007; http://www.unapcict.org/ecohub/resources/small-and-medium-enterprises-and-ict/at_download/attachment1
11. Zenger, A. and Smith, D. I., Impediments to using GIS for real-time disaster decision support. *Comput., Environ. Urban Syst.*, 2003, **27**, 123–141.
12. Indian Meteorological Department (IMD), Cyclonic storm ‘LEHAR’ over Andaman Sea: cyclone warning for Andaman & Nicobar Islands (Orange Message): BOB07/2013/02, 2013.
13. Chakravarty, N. V. K., Tripathi, K. P. and Gangwar, B., A comparative study of coastal climate with special reference to Andamans, India-I. Temperature and rainfall. *J. Andaman Sci. Assoc.*, 1987, **3**(2), 119–124.
14. Census of India, Andaman and Nicobar Islands: data sheet on rural urban breakup of population. Census Directorate, Andaman and Nicobar Islands, Port Blair, 2011; http://censusindia.gov.in/2011-prov-results/paper2/data_files/ani/Document_19.pdf
15. Dharanirajan, K., Kasinathapandian, P., Gurugnanam, B., Narayanan, R. M. and Ramachandran, S., An integrated study for the assessment of tsunami impacts: a case study of South Andaman Island, India using remote sensing and GIS. *Coast. Eng. J.*, 2006, **49**, 229–226.
16. Kafle, T. P., Hazarika, M. K., Shrestha, K. G., Prathumchai, K. and Samarakoon, L., Integration of remote sensing and GIS with flood simulation model for flood hazard mapping in the Bagmati River, Nepal. In Proceedings of New Technologies for Urban Safety of Mega Cities in Asia Phuket, Thailand, 2006.
17. Champion, G. H. and Seth, S. K., General silviculture for India. Government of India (GoI), 1968.
18. Kulkarni, S., Ecological assessment of coral reefs in Mahatma Gandhi Marine National Park, Wandoor, and Andaman & Nicobar Islands: conservation implications. Wildlife Institute of India, 2000.
19. Andrews, H. V. and Sankaran, V., Sustainable management of protected areas in the Andaman & Nicobar Islands. Andaman and Nicobar Environmental Team (ANET), Fauna and Flora International (FFI) and Indian Institute of Public Administration (IIPA), New Delhi, 2002.
20. National Horticulture Mission, Report of the Joint Inspection Team which reviewed the Andaman & Nicobar Islands during 3–4 April 2013. National Horticulture Mission Programmes, Department of Agriculture & Cooperation, GoI, 2013.

Application of fast Fourier transform in fluvial dynamics in the upper Brahmaputra valley, Assam

Siddhartha Kumar Lahiri^{1,2,*} and Rajiv Sinha²

¹Department of Applied Geology, Dibrugarh University, Dibrugarh 786 004, India

²Department of Earth Sciences, Indian Institute of Technology, Kanpur 208 016, India

Large tropical rivers such as the Brahmaputra flowing through tectonically active areas show highly variable bankline migration for the channel belt as a whole, as well as intra-bank, over different time windows due to different but non-uniform forcings. Fast Fourier transform (FFT) can be applied to identify frequency (cycles per unit length) content of bankline migration, to classify the wavelengths of different forcings and subsequently to compare the relative influence of different forcings for the trend analysis of bankline shift and width variation. This helps expand the interpretative scope of dynamics of river systems and plan mitigation strategies.

Keywords: Bankline migration, fast Fourier transform, fluvial dynamics, forcings.

THE upper reaches of the Brahmaputra River, from the 1915 confluence of three great rivers, the Lohit, the Dibang and the Siang at Kobo, up to the Mikir hills SW of the Brahmaputra valley in Assam have witnessed some of the onset spectacular riverscape changes during the last century^{1–6}. We have studied the stretch sandwiched between the NE–SW trending Himalayan Frontal Thrust (HFT) and the Naga Patkai Thrust (NPT) belt covering approximately 240 × 80 sq. km area (Figure 1). The study area was subdivided into three units: a newly formed river island (Dibru–Saikhoa Reserve Forest or ‘new Majuli’) bearing channel belt in the upstream side (unit 1), the middle connecting link (unit 2) and the ‘old Majuli’ bearing belt in the downstream side (unit 3).

Our earlier works^{7,8} have documented at least five major changes of considerable geomorphological significance in the Brahmaputra River channel during the period 1915–2005. First, the average width of the channel belt changed from 9.74 km in 1915 to 11.65 km in 1975 (i.e. 19.6% increase) and then further to 14.03 km in 2005 (44% increase compared to 1915). Secondly, during the same period, the largest colonized river island, the Majuli, eroded alarmingly and its area changed from 797.87 sq. km in 1915 to 640.5 sq. km in 1975 and then to 508.2 sq. km in 2005 – this means a reduction of 18.7% to 35.5% in terms of area compared to 1915. Thirdly, the Dibru–Saikhoa Reserve Forest, a hotspot of biodiversity,

Received 28 December 2013; revised accepted 9 September 2014

*For correspondence. (e-mail: siddharthalahiri@dibru.ac.in)

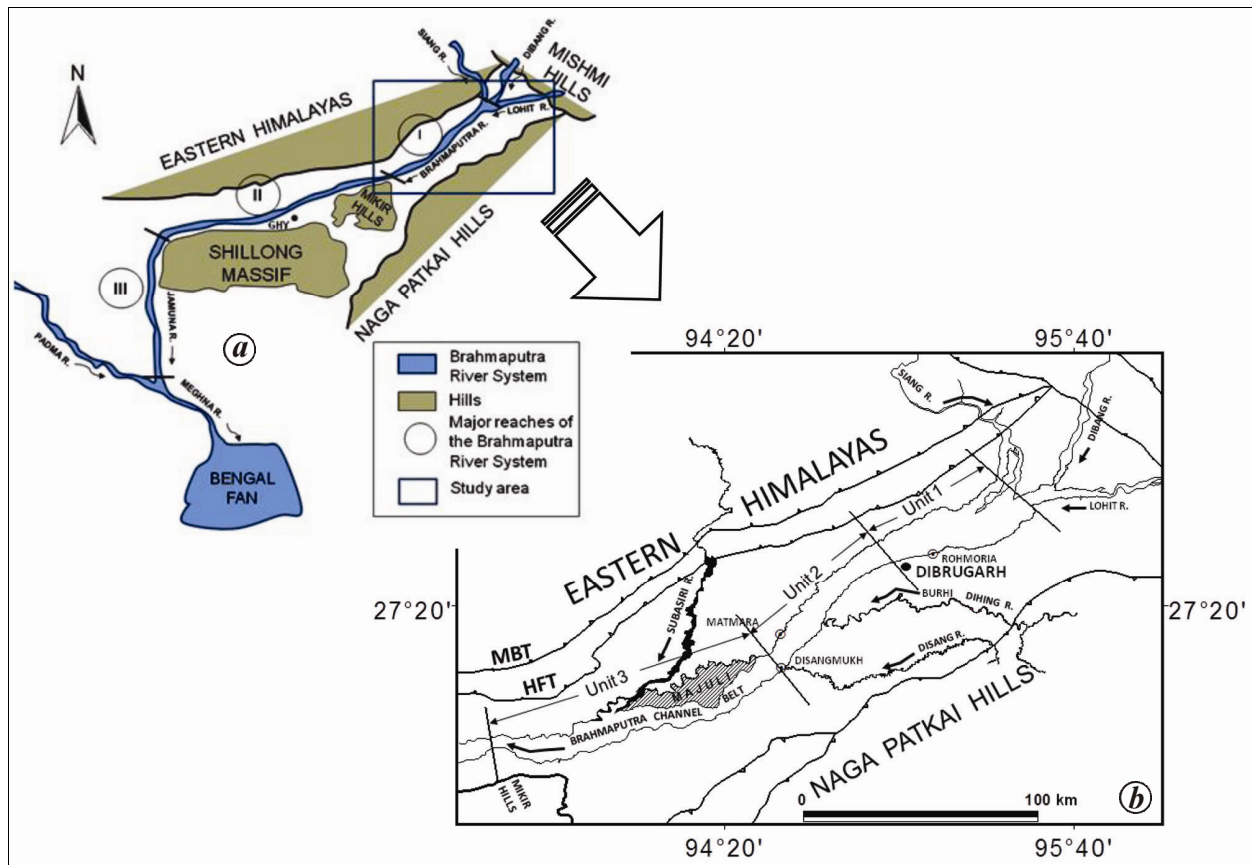


Figure 1. *a*, A cartoon (not to scale) showing three major reaches of the Brahmaputra. *b*, Reach I, located in the upper Brahmaputra valley in Assam, is divided into three units. Unit 1 is from the old confluence of three rivers, the Lohit, the Dibang and the Siang to Dibrugarh in the downstream direction. In recent times this unit experienced a large degree of bankline migration in the last one and half decades, a new island has also come up in this unit which earlier used to be the Dibru–Saikhoa Reserve Forest. Comparatively steady, Unit 2 continues up to the upper tip of the Majuli Island. Unit 3 includes the Majuli Island and extends towards the Mikir hills.

has become another Majuli-type relic island of approximately 300 sq. km area, which was earlier a part of the older floodplains of the south bank of the valley. Fourthly, the channel bar area with respect to channel area has generally been changing, suggesting variable channel aggradation/degradation during this period. Lastly, though the median position of the Brahmaputra River has not changed much during the period 1915–2005, the thalweg of the channel belt (assuming the widest channel in the planform represents the deepest) has gone through substantial change; in particular close to the lowermost part of the Majuli Island. A continuously westward migrating trend of the thalweg combined with the migration of the Subansiri River in the downstream direction in the western flank of Majuli, has accelerated the rate of erosion of the Island. These observations suggest that the ‘controls’ of different orders are influencing the channel belt of the Brahmaputra River in multifarious ways.

This communication shows that bankline migration of the Brahmaputra River in its uppermost reaches in Assam has a strong correlation with the tilt of the basin. Secondly, plano-temporal width variation of the river is

controlled by the bank migration characteristics, which in turn can be related to different orders of forcings. Although the precise geomorphic manifestations of different forcings are not understood yet, we could identify different orders of control by the application of fast Fourier transform (FFT) that gives a basis for the classification of controls on bankline migration and a means to compare the relative influence of these controls in reshaping the banklines.

Topographic maps (period 1912–1926; scale 1 : 253,440, that is, 1 inch = 4 miles and 1976; scale 1 : 250,000), satellite imageries (IRS-P6-LISS-3 images acquired on 15 December 2005 with a spatial resolution of 23.5 m) and Shuttle Radar Topographic Mission (SRTM) data (spatial resolution 90 m and vertical resolution 1 m) were georeferenced and work was done in the GIS environment with intermittent field visits. Smaller second-order reaches (unit 1: 9, unit 2: 9 and unit 3: 19), each with a spacing of 4.5–9.0 km, were selected for comparing geomorphic parameters during different times.

Large river valleys in tectonically active areas often show basin asymmetry, and this is indicative of a distinct tendency of the valley tilt⁹ (Figure 2*a*, modified from

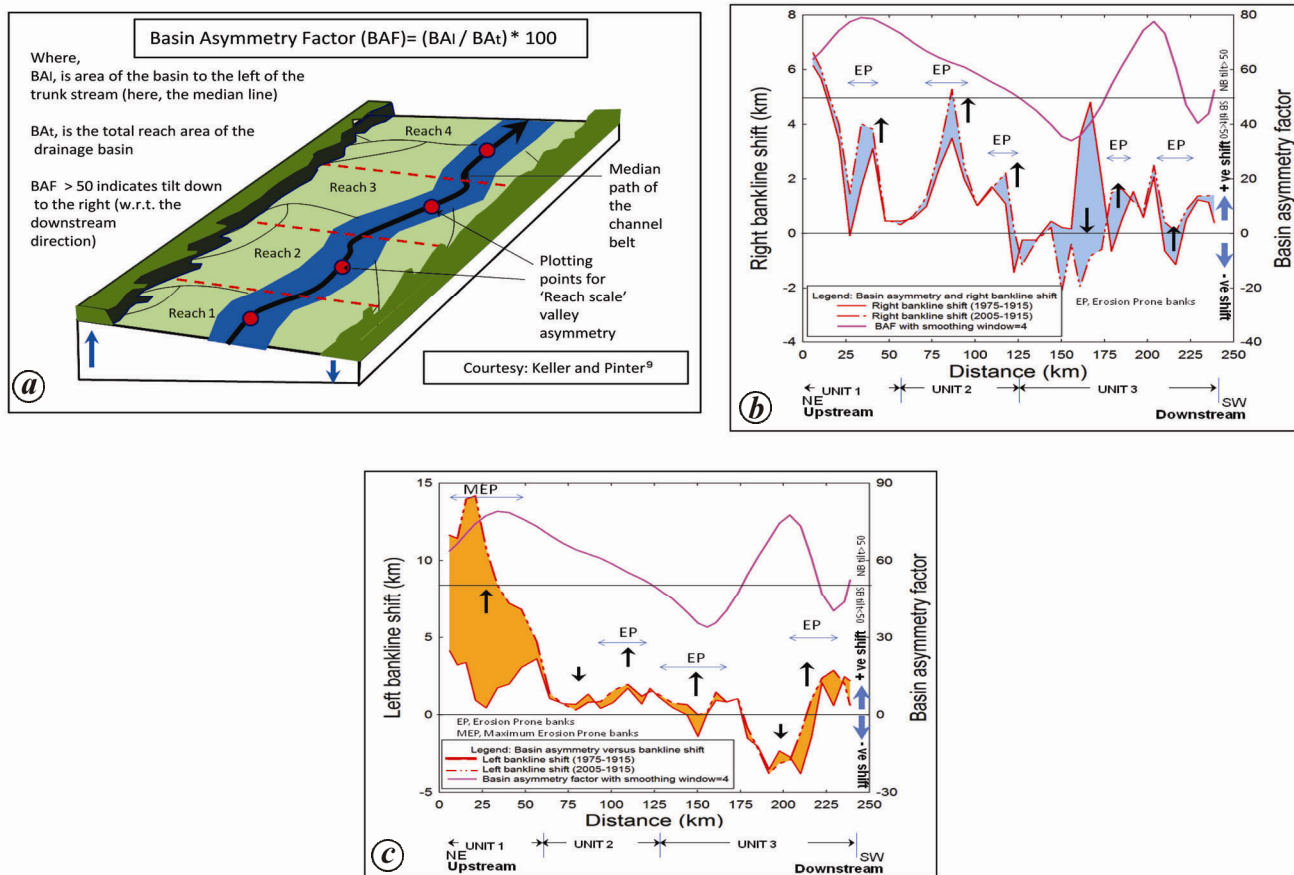


Figure 2. a, Basin asymmetry factor modified from Keller and Pinter⁹. The model shows the nature of valley tilt as a result of tectonic control. b, Comparison of basin asymmetry and right bankline shift. The shaded area between the bankline shift during 1915–1975 and 1915–2005, shows the change that took place between 1975 and 2005. The pattern of the right bankline (north bank) shift is in conformity with the trend of basin asymmetry. c, Comparison of basin asymmetry and left bankline shift. The shaded area between the bankline shift during 1915–1975 and 1915–2005, shows the change that took place between 1975 and 2005. The pattern of left bankline (south bank) shift is in partial conformity with the trend of basin asymmetry. EP, Erosion-prone bankline; MEP, Maximum erosion-prone bankline.

Keller and Pinter⁹). In this scheme of basin asymmetry measurement, a value of 50 stands for perfect symmetry and hence no tilt. Basin asymmetry was computed for 37 numbers of second-order reaches.

Since the median path of a valley-dividing channel is an established morpho-tectonic criteria⁹ for measuring valley asymmetry, and hence, the tilt direction of the valley, we extended this concept to bankline migration. Moreover, the Brahmaputra River in the study reach is quite wide, and the two banks are fed by tributaries from distinctly different hinterlands⁷. Consequently, the two banks of the Brahmaputra are likely to have differential influence of different types of forcings at different times. To identify the composition of different types of forcings on bankline migration, it is essential to know the frequency content of bankline migration (discussed in detail later) for which FFT was applied in the DPlot software. The algorithm needs equal data spacing and the number of input points (*N*) in the input record should be a power of 2. The advantage of the software is that it directly accepts the data from the Excel worksheet.

The Brahmaputra River divides the upper reaches of the Brahmaputra valley asymmetrically with the overall basin asymmetry factor (BAF) of 59. The overall valley tilt is along the eastern Himalayan margin. However, mean basin asymmetry for different units shows different values with a fast decreasing trend from 72 to 62 and then to 52. For the three segments studied, the magnitude of asymmetry varies considerably (Figure 2 b and c). Maximum asymmetry (76) is observed in unit 1 and minimum asymmetry (38) in unit 3. A stretch of about 54 km, located mostly within unit 3 shows a value of <50 for asymmetry factor indicating dominant influence of the NPT compared to eastern HFT on the basin-scale tilting. The median path of the Brahmaputra River (excluding the Majuli Island) in the overall stretch is almost straight with slight temporal variation in sinuosity from 1.09 to 1.1 in a span of 90 years (1915–2005). When we compare the differences in the bankline shift between the two periods 1915–1975 and 1915–2005 and thereby identify the erosion-prone (EP) zones with basin asymmetry, it is observed that the north bankline (right bank) shift

(Figure 2 b) is in conformity with the basin asymmetry. A positive excursion (bankline moving away from the median path of the channel belt) of the north bankline emphasizes a tilt towards the eastern Himalayan side of the basin, whereas negative excursion (bankline moving towards the median path of the channel belt) indicates a tilt towards the Naga Patkai side. On the contrary, a negative excursion for the south bankline should emphasize a tilt towards the eastern Himalayan side and positive excursion a tilt towards the Naga Patkai side. The pattern of left bankline (south bank) shift (Figure 2 c) is in partial conformity with the trend of basin asymmetry.

Even for drastic bankline migration, there may not be any significant width variation of the channel belt. However, for our specific study area, trend analysis of the width variation shows a distinct relationship with the nature of bankline migration of the channel belt (Figure 3). Widening of unit 1 seems to be controlled by the south bankline shift (SBS), while that of unit 2 seems to be controlled by the north bankline shift (NBS). Unit 3 presents a complex situation. First, there is a narrowing which is being controlled by the NBS followed by a stretch that practically shows no change. Further downstream, there is again a narrowing followed by widening, both controlled by the SBS. The north bank of the Brahmaputra River which is closer to the eastern HFT should be more affected by the Himalayan thrust belt tectonics. As the mountain-fed Brahmaputra River is too wide in proportion to the width of the valley, the NPT belt, besides influence from the HFT, should also influence the south bank of the Brahmaputra channel belt. Thus,

bankline migration and width variation of the channel belt are affected by competing tectonics of the HFT and NPT.

Though the mathematical operation of FFT is usually meant for a transform of functions from time domain to frequency domain^{10,11}, the same principle is applied here to replace discrete cumulative time by discrete cumulative distance and the amplitude term is replaced by the magnitude of bankline shift (A_b). Thus, FFT will give a different kind of frequency content (cycles/unit length) of the bankline shift [$B(f_n)$], which can provide us a scheme of classifying the nature of forcings in shaping the bankline (see Box 1).

Box 1. Fast Fourier transform for computing the frequency content of bankline migration.

Given a variable function of amplitude of bankline migration with distance $A_b(d_k)$ with N consecutive sampled values, the fast Fourier transform implementation used by DPlot software for the present purpose, calculates the corresponding function in the frequency domain as

$$B(f_n) = \frac{1}{N} \sum_{k=0}^{N-1} A_b(d_k) e^{2\pi kn/N},$$

where $d_k = k\Delta$, $f_n = 0 < K < 1/2\Delta$, Δ the distance-interval, $1/2\Delta$ the maximum sampling frequency or twice the Nyquist frequency that can be reproduced without 'aliasing' and K the Intermediate frequencies between zero and the maximum.

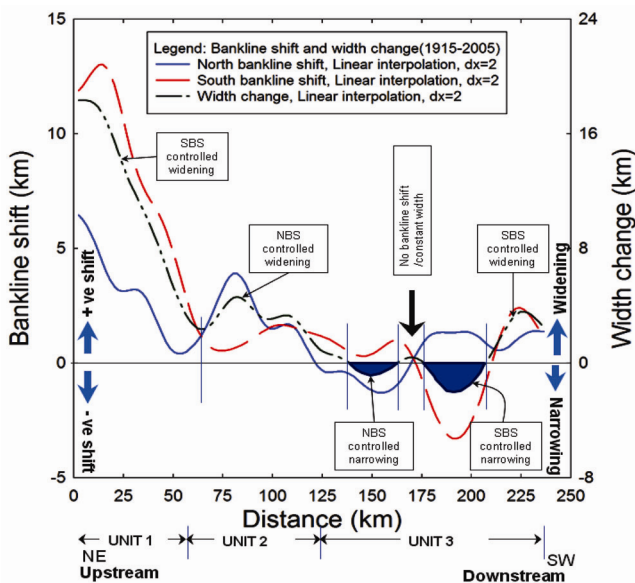


Figure 3. Relationship between bankline shift and width variation. Unit 1: widening is controlled by the south bankline shift. Unit 2: widening is controlled by the north bankline shift. Unit 3: Mixed nature of controls.

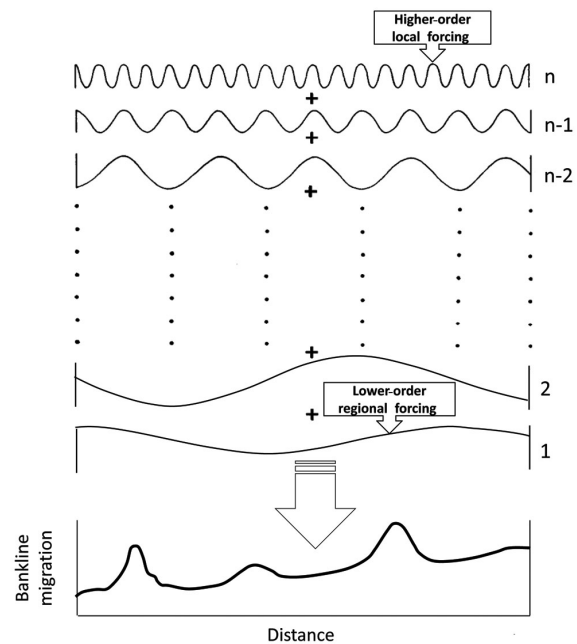


Figure 4. Replication of bankline migration as a cumulative effect of forcings of different order.

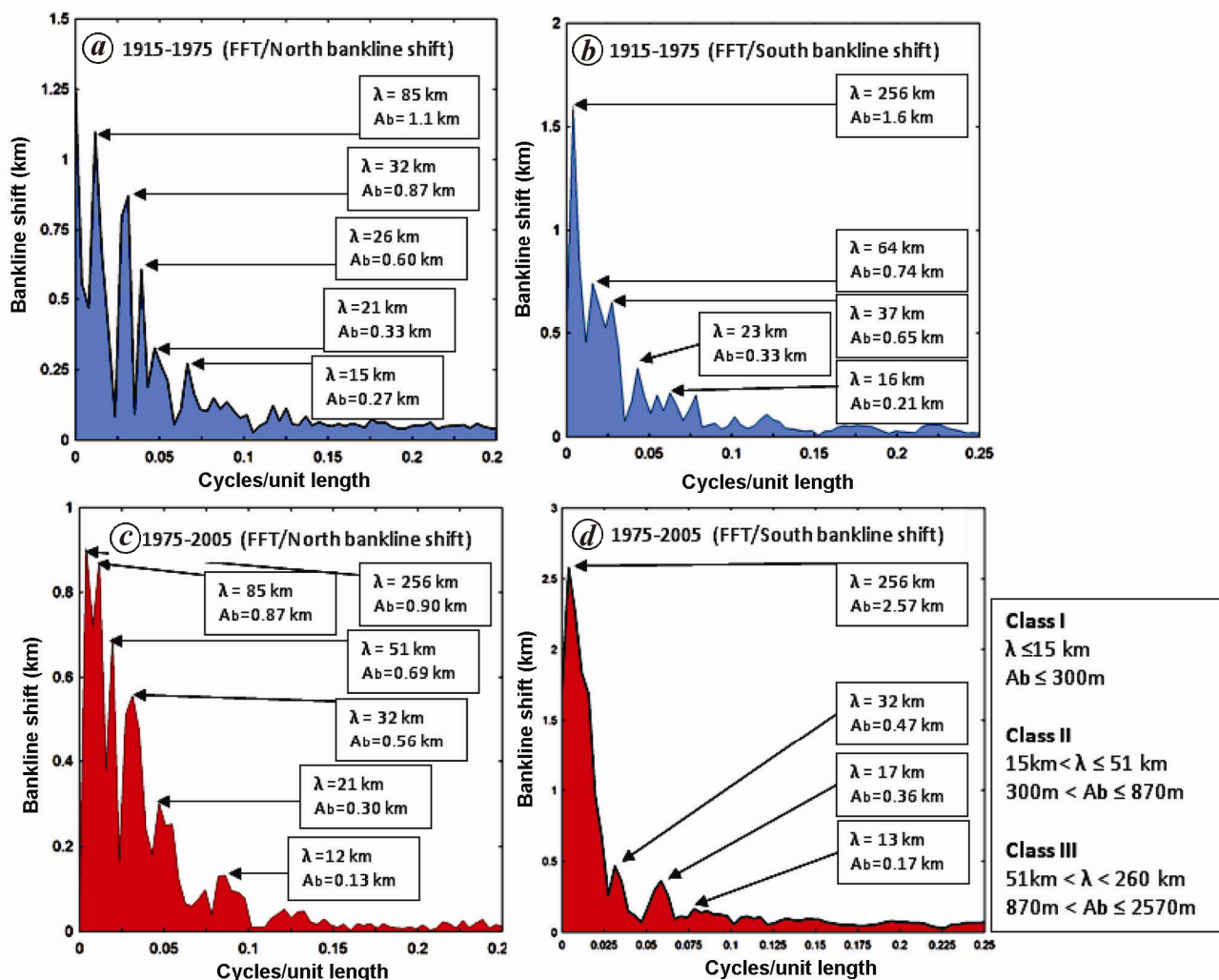


Figure 5. Fast Fourier transform of bankline shifts for the north and south banks during two different periods, 1915–1975 and 1975–2005. Presence of three classes of forcings having different wave bands is identified. Some of the prominent ‘peaks’ are also identified. It is observed that south bankline shifts during 1975–2005 are free from the forcings of class II.

Bankline migration of a river flowing over tectonically active landscape can be assumed to represent a superposition of forcings having different orders expressed in the form of sinusoidal waves of variable lengths and frequencies (Figure 4). Thus, large-scale tectonic controls having regional dimension will represent long wavelength, low frequency waves. In case of a dominant control of localized origin, the wavelength will be shorter and frequency will be higher.

Moreover, this helps to discriminate whether the principal cause of change observed at a particular reach is the fallout of the local control or regional control. Additionally, whether changes observed in the bankline shifts of two banks of a big river are caused due to the same forcings or not can be compared. Figure 5 shows the results of FFT applied on bankline shift.

It is observed that the trend of bankline shift can be divided into at least three classes for the 240 km stretch

of the Brahmaputra channel belt in the upper reaches of the river system for the period 1915–2005. Class I represents the short wavelength ($\lambda = (1/f)$, f is cycles/unit length) and high frequency forcings with wavelengths equal to or less than 15 km. These are responsible for bankline shift of the order of less than or equal to 300 m. Class II represents the medium wavelength forcings with wavelengths greater than 15 km and less than or equal to 51 km. These are responsible for the bankline shifts of the order of greater than 300 m and lesser than or equal to 870 m. Class III represents the long wavelength and low frequency forcings with wavelengths greater than 51 km and less than 260 km. These are responsible for the bankline shifts greater than 870 m and less than or equal to 2570 m.

Based on our understanding of the fluvial processes in the region^{7,8}, we propose the following scenarios to represent these classes.

Class I: Changing thalweg or shifting of the widest channel within the channel belt; second-order variability in the channel aggradation/degradation sites.

Class II: Advancing blind faults of local as well as regional proportion from the frontal thrust belts of orogeny towards the valley.

Class III: Co-seismic subsidence of some of the first-order morpho-tectonic zones of depression and effective change in the overall valley tilt.

A significant difference is observed in the frequency content of the bankline shift of the north and south banks in the upper reaches of the Brahmaputra River. Some of the prominent peaks are shown for both the north and south bankline shifts (Figure 5). The study shows that the south bankline migration during 1915–1975 has a greater presence of class I frequency content ($\lambda \leq 15$ km and bankline migration ≤ 300 m) and a sharp peak of class III event ($\lambda = 256$ km and bankline migration greater than 1.5 km). The situation remains more or less similar during 1975–2005 with a difference in the class II forcings, which shows that the number of peaks reduces from 6 to 2. On the other hand, the north bankline migration shows the presence of all three classes of forcings and there is a remarkable temporal consistency for both the periods considered in the present discussion. We therefore suggest that the eastern Himalayan frontal thrust is influencing the migration characteristics of the north bankline of the Brahmaputra channel belt consistently at a decadal scale. However, this is not so prominent for the south bankline migration. For the south bankline migration during the period 1915–2005, the first-order morpho-tectonic subsidence seems to be playing a more dominant role.

Riverscape variability in tectonically active foreland basins can be fast enough to be observed by decadal-scale monitoring through maps and satellite imageries. Besides documenting the changes in various geomorphologic parameters, it has become important to quantify and understand the mechanisms, the nature of ‘controls’ and the relative importance of different ‘controls’ in different reaches of the river systems. This can help develop predictive models of river dynamics, landform evolution and sediment budgeting in smaller reaches. A multidisciplinary approach that includes application of FFT for the trend analysis of the bankline migration was used in the upper reaches of the Brahmaputra channel belt in Assam. It was observed that the nature of valley tilt and bankline migration had a definite correlation. Width variation of the channel belt shows a distinct correlation with the nature of bankline migration. The frequency content of the north bankline shift shows a temporal consistency between two periods 1915–1975 and 1975–2005 respectively indicating unchanging characteristics of different classes of forcings. During the same period, the south bankline of the Brahmaputra channel belt shows a significant change in the frequency content of the three classes

of forcings, which is probably due to the increasing influence of the first-order morphotectonic changes related to co-seismic–interseismic structural readjustments in the foreland areas of the valley.

1. Kotoky, P., Bezbaruah, D. and Sarma, J. N., Erosion activity on Majuli – the largest river island in the world. *Curr. Sci.*, 2003, **84**(7), 929–932.
2. Kotoky, P., Bezbaruah, D., Baruah, J. and Sarma, J. N., Nature of bank erosion along the Brahmaputra River channel, Assam, India. *Curr. Sci.*, 2005, **88**, 634–640.
3. Sarma, J. N. and Phukan, M. K., Origin and some geomorphological changes of the river island Majuli of the Brahmaputra in Assam, India. *Geomorphology*, 2004, **60**, 1–19.
4. Sarma, J. N., Fluvial process and morphology of the Brahmaputra River in Assam, India. In *Geomorphology* (eds Latrubesse, E. M., Stevau, J. C. and Sinha, R.), 2005, vol. 70, pp. 226–256.
5. Sarma, J. N. and Phukan, M. K., Bank erosion and bankline migration of the river Brahmaputra in Assam, India, during the twentieth century. *J. Geol. Soc. India*, 2006, **68**, 1023–1036.
6. Singh, S. K., Spatial variability in erosion in the Brahmaputra basin: causes and impacts. *Curr. Sci.*, 2006, **90**, 1272–1276.
7. Lahiri, S. K. and Sinha, R., Tectonic controls on the morphodynamics of the Brahmaputra River system in the upper Assam valley, India. *Geomorphology*, 2012, **169–170**, 74–85.
8. Lahiri, S. K. and Sinha, R., Morphotectonic evolution of the Majuli Island in the Brahmaputra valley of Assam, India inferred from geomorphic and geophysical analysis. *Geomorphology*, 2014; doi:10.1016/j.geomorph.2014.04.032.
9. Keller, E. A. and Pinter, N., *Active Tectonics – Earthquakes, Uplift, and Landscape*, Prentice Hall, London, 2002, 2nd edn.
10. Cooley, J. W. and Tukey, J. W., An algorithm for the machine calculation of complex Fourier series. *Math. Comput.*, 1965, **19**, 297–301.
11. Press, W. H., Teukolsky, S. A., Vetterling, W. T. and Flannery, B. P., *Fast Fourier transform*. In *Numerical Recipes: The Art of Scientific Computing*, Cambridge University Press, New York, 2007, 3rd edn; ISBN 978-0-521-88068-8

ACKNOWLEDGEMENTS. We thank IIT Kanpur and Dibrugarh University, Assam for support and USGS website for providing the DEM data from the SRTM source. We also thank the India Office Library and Records, London, UK, for providing the topographic map of the study area prepared during the 1912–1926 seasons.

Received 24 May 2014; revised accepted 17 September 2014